

Spin relaxation in n -type ZnO quantum wells

C. Lü and J. L. Cheng*

*Hefei National Laboratory for Physical Sciences at Microscale and Department of Physics,
University of Science and Technology of China, Hefei, Anhui, 230026, China*

(Dated: November 2, 2018)

We perform an investigation on the spin relaxation for n -type ZnO (0001) quantum wells by numerically solving the kinetic spin Bloch equations with all the relevant scattering explicitly included. We show the temperature and electron density dependence of the spin relaxation time under various conditions such as impurity density, well width, and external electric field. We find a peak in the temperature dependence of the spin relaxation time at low impurity density. This peak can survive even at 100 K, much higher than the prediction and measurement value in GaAs. There also exhibits a peak in the electron density dependence at low temperature. These two peaks originate from the nonmonotonic temperature and electron density dependence of the Coulomb scattering. The spin relaxation time can reach the order of nanosecond at low temperature and high impurity density.

PACS numbers: 72.25.Rb, 73.21.Fg, 71.10.-w

I. INTRODUCTION

Much attention has been devoted to the spin degree of the freedom of carriers in the zinc oxide (ZnO) with wurtzite structure in the last few years,¹ partly because of the very long spin relaxation time (SRT)^{2,3,4} and the prediction that ZnO can become ferromagnetic with a Curie temperature above room temperature if doped with manganese.⁵ However, only few works investigate on the spin dynamics properties of ZnO: Experimentally, Ghosh *et al.*² investigated the electron spin properties in n -type bulk ZnO and discovered the electron spin relaxation time varying from 20 ns to 190 ps when the temperature increased from 10 to 280 K. Liu *et al.*³ measured the SRT in colloidal n -type ZnO quantum dots could be as long as 25 ns at room temperature by electron paramagnetic resonance spectroscopy. Theoretically, Harmon *et al.* calculated the SRT in bulk material in the framework of a single-particle model.⁶ However, a theoretical investigation on the SRT in quantum wells (QWs) is still rare, which is our task in the present paper.

The spin relaxation can be induced by the following mechanisms: (i) D'yakonov-Perel'(DP) spin relaxation mechanism,⁷ which is revealed to be the dominant mechanism in n -doped semiconductors.^{8,9} For n -doped ZnO QW, the spin-orbit coupling (SOC) is at least one order of magnitude weaker compared with that of the well studied semiconductor GaAs^{10,11}, a simple estimation shows that the criterion of the strong scattering⁹ is always satisfied even the momentum scattering is also weaker than that in GaAs due to the larger effective mass m^* . Therefore the DP mechanism here can be described by the motional narrowing picture¹² qualitatively and the induced SRT is

$$\tau \propto \frac{1}{\langle \Omega_{\mathbf{k}}^2 \rangle \tau_p}, \quad (1)$$

with τ_p standing for the momentum scattering time and $\langle \Omega_{\mathbf{k}}^2 \rangle$ for the inhomogeneous broadening induced by the

SOC. As pointed out first by Wu *et al.*^{13,14,15} and then by Glazov and Ivchenko,¹⁶ the electron-electron scattering has important contribution to the spin relaxation process. Therefore τ_p used in Eq. (1) should be revised as $\tau_p^* = \left[(\tau_p)^{-1} + (\tau_p^{ee})^{-1} \right]^{-1}$ to include the electron-electron momentum relaxation time τ_p^{ee} .^{8,9,13,14,15,16,17,18} (ii) Elliott-Yafet mechanism.¹⁹ The revised criterion in Eq. (22) of Refs. [8] gives $\Theta \approx 340$ eV, which means the Elliott-Yafet mechanism is negligible compared with the DP mechanism⁶ due to the small spin split off energy, the large band gap, and the large m^* . (iii) Bir-Aronov-Pikus mechanism,²⁰ which is always unimportant in n -doped semiconductor.^{8,9} Therefore, we only investigate the SRT induced by the DP mechanism for n -type ZnO QWs in the following.

In this paper, we quantitatively calculate the SRT for n -type ZnO QWs by using the fully microscopic spin kinetic Bloch equation (KSBE) approach, which has been successfully used in investigating the spin relaxation in QWs^{9,13,14,15,21} and in bulk semiconductors.^{8,22} With all the relevant scattering included, the influence of temperature, electron density, impurity density, well width and electric field on the SRT are studied detailedly. The temperature and density dependence of the SRT is shown to be nonmonotonic, and we find that the SRT increases with the electric field monotonically.

This paper is organized as follows: In Sec. II we describe our model and the KSBEs. Our numerical results are presented in Sec. III. We conclude in Sec. IV.

II. MODEL AND KSBES

We start our investigation from a n -doped ZnO QW of well width a grown in (0001) direction, considered to be z axis. Due to the confinement of QW, the momentum states along z -axis is quantized by subband index n . With the momentum vector $\mathbf{k} = (k_x, k_y)$ and the

spin index σ , the electron Hamiltonian can be written as $H_e = \sum_{\substack{n\mathbf{k} \\ \sigma_1\sigma_2}} \{\mathcal{E}_{n\sigma_1\sigma_2\mathbf{k}} - e\mathbf{E} \cdot \mathbf{R}\delta_{\sigma_1\sigma_2}\} a_{n\sigma_1\mathbf{k}}^\dagger a_{n\sigma_2\mathbf{k}} + H_I$.

Here $\mathcal{E}_{n\sigma_1\sigma_2\mathbf{k}} = \varepsilon_{n\mathbf{k}}\delta_{\sigma_1\sigma_2} + [\mathbf{h}_R(\mathbf{k}) + (\mathbf{h}_D)_n(\mathbf{k})] \cdot \boldsymbol{\sigma}_{\sigma_1\sigma_2}$ with $\varepsilon_{n\mathbf{k}} = \frac{\mathbf{k}^2}{2m^*} + \frac{\langle k_z^2 \rangle_n}{m^*}$ is the energy spectrum, $\mathbf{R} = (x, y)$ is the position, the effective magnetic field given by the Rashba due to the intrinsic wurtzite structure inversion asymmetry and Dresselhaus SOC can be written as:¹⁰

$$\begin{aligned} \mathbf{h}_R(\mathbf{k}) &= \alpha_e(k_y, -k_x, 0), \\ (\mathbf{h}_D)_n(\mathbf{k}) &= \gamma_e(b\langle k_z^2 \rangle_n - k_{\parallel}^2)(k_y, -k_x, 0), \end{aligned} \quad (2)$$

with α_e , γ_e and b standing for the SOC coefficients. $\langle k_z^2 \rangle_n = \frac{\hbar^2 \pi^2 n^2}{a^2}$ is the subband energy in a hard-wall confinement potential. The scattering Hamiltonian H_I includes all the scatterings, such as electron-nomagnetic impurity scattering, electron-phonon scattering, and electron-electron scattering.

We construct the KSBEs in the collinear statistics by using the non-equilibrium Green function method as follows:^{13,14,15,23,24}

$$\partial_t \rho_{\mathbf{k}} - e\mathbf{E} \cdot \nabla_{\mathbf{k}} \rho_{\mathbf{k}} = \partial_t \rho_{\mathbf{k}}|_{\text{coh}} + \partial_t \rho_{\mathbf{k}}|_{\text{scat}}. \quad (3)$$

The density matrix $\rho_{\mathbf{k}}$ for momentum \mathbf{k} is a matrix with matrix elements $[\rho_{\mathbf{k}}]_{n_1\sigma_1;n_2\sigma_2}$ which include all the coherence between different subbands and different spins. The second terms on the left-hand side of the kinetic equations describe the electric field \mathbf{E} driven effect. $\partial_t \rho_{\mathbf{k}}|_{\text{coh}}$ is the coherent term. $\partial_t \rho_{\mathbf{k}}|_{\text{scat}}$ denotes the scattering, including the electron-impurity, the electron-phonon, as well as the electron-electron scattering. The expressions for these terms are given in Appendix A.

Before we give our numerical results, the qualitative analysis of the DP mechanism due to the electron-electron scattering can be made at strong scattering limit. The perturbation theory shows the effective electron-electron momentum scattering time τ_p^{ee} in degenerate and nondegenerate limits satisfies²⁷

$$\frac{1}{\tau_p^{ee}} \propto \begin{cases} T^2 N_e^{-1}, & \text{for } T \ll T_F, \\ T^{-1} N_e, & \text{for } T \gg T_F, \end{cases} \quad (4)$$

which has nonmonotonic temperature T and electron density N_e dependence as the electron gas undergoes the transition from the degenerate case to the nondegenerate case at the Fermi temperature T_F . As the SOC in ZnO QWs mainly depends on \mathbf{k} linearly, the inhomogeneous broadening is given by

$$\langle \Omega_{\mathbf{k}}^2 \rangle \propto \begin{cases} N_e, & \text{for } T \ll T_F, \\ T, & \text{for } T \gg T_F. \end{cases} \quad (5)$$

Then by Eq. (1), the electron-electron scattering contributes to the SRT τ as¹⁸

$$\tau \propto \begin{cases} T^2 N_e^{-2}, & \text{for } T \ll T_F, \\ T^{-2} N_e, & \text{for } T \gg T_F. \end{cases} \quad (6)$$

The SRT is expected to reach a minimum in T dependence or a maximum in N_e dependence, and the location of the extreme points satisfy $T \approx T_F$.

III. NUMERICAL RESULTS

We numerically solve the KSBEs for the spin density matrix ρ , from which we obtain the time evolution of the spin polarization along z -direction:¹⁴

$$P_z(t) = \sum_{n,\mathbf{k}} \{[\rho_{\mathbf{k}}]_{n\uparrow;n\uparrow}(t) - [\rho_{\mathbf{k}}]_{n\downarrow;n\downarrow}(t)\} / N_e, \quad (7)$$

where N_e is the total electron density. The SRT τ is extracted from the exponential decay of the envelope of $P_z(t)$. The initial condition at $t = 0$ is taken to be

$$[\rho_{\mathbf{k}}]_{n_1\sigma_1;n_2\sigma_2} = f_{T,\mu_{\sigma_1}}(\mathbf{k}) \delta_{n_1 n_2} \delta_{\sigma_1 \sigma_2}. \quad (8)$$

Here $f_{T,\mu}(\mathbf{k}) = [1 + e^{(\varepsilon_{\mathbf{k}} - \mu)/(k_B T)}]^{-1}$ gives the Fermi-Dirac distribution. The spin dependent chemical potential μ_{σ} is chosen to satisfy $P(0) = 2.5\%$. The electron density and the quantum well width are taken as $N_e = 4 \times 10^{11}/\text{cm}^2$ and $a = 10$ nm respectively unless otherwise specified. All used parameters are listed in Table I. In the calculation, only the lowest two subbands are taken into account.

TABLE I: Material parameters used in the calculation (from Ref. 28 unless otherwise specified).

κ_{∞}	3.7	κ_0	7.8
m_e/m_0	0.25	v_1 (km/s)	6.08
v_3 (km/s)	6.09	v_4 (km/s)	2.73
v_6 (km/s)	2.79	b	3.91 ^a
γ_e (eVÅ ³)	0.33 ^a	α_e (meVÅ)	1.1 ^b
e_{15} (V/m)	-0.35×10^9	e_{33} (V/m)	1.56×10^9

^a Ref. [10];

^b Ref. [11].

A. Temperature dependence

We now study the temperature dependence of the SRT presented in Fig. 1 for different impurity densities. The results are similar to that in GaAs QWs^{9,29} and can be understood as follows: (i) The SRT always increases with the impurity density N_i . It is because the system is in the strong scattering regime as stated above due to the weak SOC, thus the spin relaxation can be explained by the motional narrowing picture qualitatively^{9,12}, and the additional scattering leads to longer SRT. (ii) The electron-phonon scattering is shown to be negligible over the whole temperature regime by comparing the temperature dependence of SRT with (solid curve with \blacktriangle)

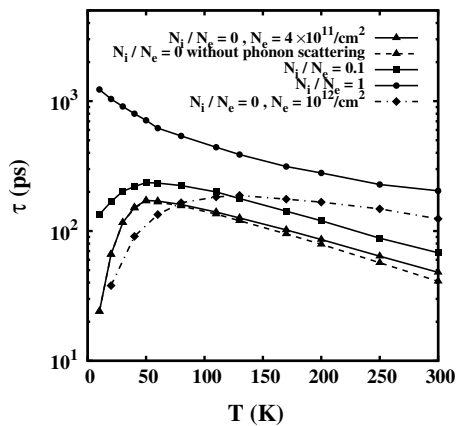


FIG. 1: SRT τ vs. temperature T at different impurity densities. The dashed curve is obtained from the calculation of excluding the electron-phonon scattering.

or without (dashed curve with \blacktriangle) the electron-phonon scattering for the impurity free case in the same figure. (iii) The SRT presents a peak at very low N_i . In these cases, the electron-electron scattering is the dominant scattering, therefore, as shown in Eq. (6), the SRT shows a maximum and the transition temperature T_F for $N_e = 4 \times 10^{11} / \text{cm}^2$ is about 44 K, which is agree with our numerical results. (iv) When the impurity density is high enough such as $N_i = N_e$, the SRT decreases monotonically with T . In this case the total scattering is mainly determined by the impurity scattering, which depends weakly on the temperature. However, the inhomogeneous broadening from the DP term increases with the temperature, and results in shorter SRT.

For GaAs QWs, the temperature peak of the SRT can only be observed at low electron density (*i.e.* low transition temperature) and low impurity density^{9,29}, because the electron-phonon scattering becomes strong enough to destroy the nonmonotonic T dependence of the scattering time induced by the electron-electron scattering. Such case can be avoid in ZnO QWs, in which the electron-phonon scattering is always pretty weak due to the large optical phonon energies (~ 800 K). Thus the temperature peak can be found even for high electron density samples. One can easily find from the chained curve in Fig. 1, which is calculated with parameters $N_e = 10^{12} / \text{cm}^2$ and $N_i = 0$, that the peak moves to $T \sim 100\text{K}$. Therefore, the high mobility ZnO QW is a good system for studying the electron-electron scattering.

B. Doping and well width dependence

Then we investigate the density dependence of the SRT at different temperatures and impurity densities. In Fig. 2 (a) we plot the SRT as a function of the electron density with $T = 20$ K. One can see that for the low impurity density case, the SRT reaches a maximum at $N_e \approx 2 \times 10^{11} \text{ cm}^{-2}$, which has been pointed

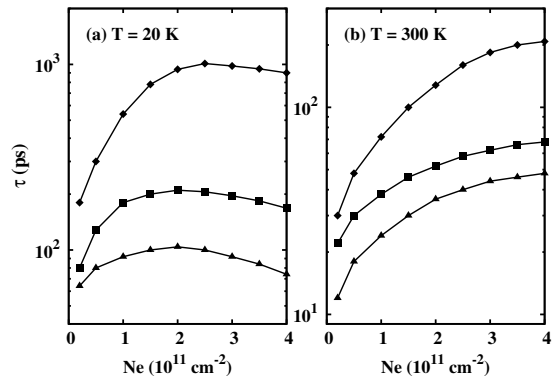


FIG. 2: SRT vs. the electron density with different impurity densities and temperatures. (a) $T = 20$ K; (b) $T = 300$ K. \blacktriangle : $N_i/N_e = 0$; \blacksquare : $N_i/N_e = 0.1$; \blacklozenge : $N_i/N_e = 1$.

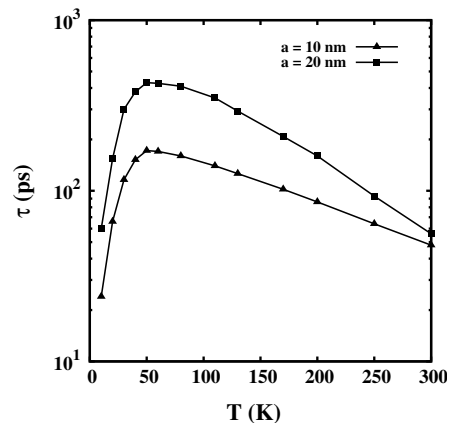


FIG. 3: SRT vs. the temperature at different quantum well widths.

out in n -type bulk III-V semiconductors^{8,22}. It originates from the transition from the nondegenerate electron gas to the degenerate electron gas and can be well explained by Eq. (6). Our calculation gives the transition density of $2 \times 10^{11} \text{ cm}^{-2}$, corresponding $T_F \sim 22$ K, close to the lattice temperature of 20 K. For the case of $N_i = N_e$, the electron-impurity scattering time has the same N_e dependence as that for electron-electron scattering: in the nondegenerate regime, $\frac{1}{\tau_{pi}} \propto N_i \langle U_q^2 \rangle$, in which $\langle U_q^2 \rangle$ changes little; in the degenerate regime, $\frac{1}{\tau_{pi}} \sim N_i U_{kf}^2 \propto N_e / k_F^4 \propto N_e^{-1}$. Consequently, the peak still exists and is almost at the same position. In comparison, the SRT as a function of N_e with $T = 300$ K is plotted in Fig. 2 (b). In this case, one finds that the SRT increases monotonically with N_e . This could be easily understood for that $T_F \ll T$ is satisfied and it is in the nondegenerate regime, in which the SRT increases with density as discussed above.

We further show the effect of quantum well width on the spin relaxation. In Fig. 3 the SRTs versus temper-

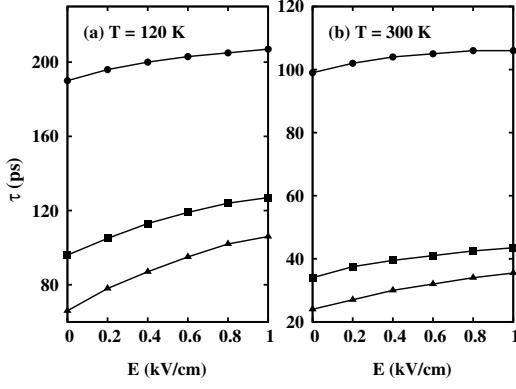


FIG. 4: SRT *vs.* the electric field at different temperature and impurity densities. \blacktriangle : $N_i/N_e = 0$; \blacksquare : $N_i/N_e = 0.1$; \bullet : $N_i/N_e = 1$.

ature at well widths $a = 10$ nm and 20 nm are plotted respectively. Both the SOC and the scattering^{17,18} depend on the quantum well width. However, comparing to the weak well width dependence of the scattering, the fast decrease of $\langle k_z^2 \rangle$ in the DP term with a dominates and so the SRT increases with well width.

C. Electric field dependence

Then we investigate the electric field dependence of the SRT at different temperatures and impurity densities. In Fig. 4 we plot the SRT as a function of the electric field for different T . The electric field is applied along the x axis. One can see that the SRT increases monotonically for both low temperature and high temperature cases. According to the previous investigation¹⁵, the electric field will enhance both the momentum scattering due to the hot-electron effect, and the inhomogeneous broadening due to the drift of the electron distribution to larger \mathbf{k} states. These two effects are competing effects for the SRT: the former tends to enhance the SRT while the later tends to suppress it.¹⁵ For SOC with linear \mathbf{k} dependence, the hot-electron effect dominates,⁸ thus the SRT always increases with E .

IV. CONCLUSION

In conclusion, we have investigated the spin relaxation for n -type ZnO (0001) QWs by numerically solving the KSBSs with all the relevant scattering explicitly included. It is shown that the electron-phonon scattering is pretty weak in ZnO QWs, while the Coulomb scattering always plays an important role. Therefore the ZnO QW is a good carrier to study the electron-electron scattering. We find there exists a peak of SRT both in the temperature dependence for a given electron density at low impurity density and in the electron density dependence at low

temperature. Both these two peaks originate from the different temperature and electron density dependence of τ_p^{ee} in degenerate and non-degenerate case. Compared with the same effect in III-V semiconductor,^{8,9,22,29} this peak position can occur at the temperature as high as 100 K and is easier to observe in experiments due to the weak electron-phonon scattering. When the impurity density is high, the peak in the temperature dependence disappears and the SRT decreases with temperature monotonously. Moreover, the peak in the electron density dependence moves to larger electron density which is beyond the scope of our interest when the temperature is high. We also investigate the hot-electron effect and show that the SRT always increases with the electric field. It is also shown that the SRT reaches the order of nonosecond at low temperature and high impurity density.

Acknowledgments

The authors would like to thank M.W. Wu for proposing the topic as well as the directions during the investigation. This work was supported by the Natural Science Foundation of China under Grant No. 10725417, the National Basic Research Program of China under Grant No. 2006CB922005, and the Knowledge Innovation Project of the Chinese Academy of Sciences. J.L.C was partially supported by China Postdoctoral Science Foundation.

APPENDIX A: EXPRESSIONS FOR KINETIC BLOCH EQUATIONS

Here we write the expressions for the coherent terms and the scattering terms in the kinetic Bloch equations. The coherent terms in Eq. (3) can be written as

$$\partial_t \rho_{\mathbf{k}} \Big|_{\text{coh}} = -i \left[E_e(\mathbf{k}) + \sum_{\mathbf{Q}} \mathbf{V}_{\mathbf{Q}} \mathbf{I}_{\mathbf{q}_z} \rho_{\mathbf{k}-\mathbf{q}} \mathbf{I}_{\mathbf{q}_z}, \rho_{\mathbf{k}} \right], \quad (\text{A1})$$

where $[A, B] = AB - BA$ denotes the commutator. $[E_e(\mathbf{k})]_{n_1 \sigma_1; n_2 \sigma_2} = \mathcal{E}_{n_1 \sigma_1 \sigma_2 \mathbf{k}} \delta_{n_1 n_2}$. The Coulomb Hartree-Fock term, which is always negligible for small spin polarization,^{14,21} is also included. The form factor I_{q_z} is also a matrix with matrix elements

$$[I_q]_{n_1 \sigma_1; n_2 \sigma_2} = iaq \delta_{\sigma_1, \sigma_2} [e^{iaq} \cos \pi(n_1 - n_2) - 1] \times \left[\frac{1}{\pi^2(n_1 - n_2)^2 - a^2 q^2} - \frac{1}{\pi^2(n_1 + n_2)^2 - a^2 q^2} \right]. \quad (\text{A2})$$

The statically screened Coulomb potential in the random-phase approximation (RPA) reads²³ $V_{\mathbf{Q}} = \frac{v_{\mathbf{Q}}}{\epsilon(\mathbf{q})}$ with the dielectric function $\epsilon(\mathbf{q}) = 1 - \sum_{\substack{q_z, \mathbf{k} \\ n_1; n_2}} v_{\mathbf{Q}} |[I_{q_z}]_{n_1; n_2}|^2 \frac{f_{\sigma}(\epsilon_{n_1, \mathbf{k}+\mathbf{q}}) - f_{\sigma}(\epsilon_{n_2, \mathbf{k}})}{\epsilon_{n_1, \mathbf{k}+\mathbf{q}} - \epsilon_{n_2, \mathbf{k}}}$ and $\mathbf{Q} = (q_x, q_y, q_z)$. The bare Coulomb potential is $v_{\mathbf{Q}} = 4\pi e^2 / Q^2$. $f_{\sigma}(\epsilon_{n, \mathbf{k}}) = [\rho_{\mathbf{k}}]_{n\sigma; n\sigma}$.

The scattering terms in Eq. (3) can be written as $\partial_t \rho_{\mathbf{k}}|_{\text{scat}} = \partial_t \rho_{\mathbf{k}}|_{\text{im}} + \partial_t \rho_{\mathbf{k}}|_{\text{ph}} + \partial_t \rho_{\mathbf{k}}|_{\text{ee}}$ in the Markovian limit with

$$\begin{aligned}
\partial_t \rho_{\mathbf{k}}|_{\text{im}} &= \pi N_i \sum_{\mathbf{Q}, n_1, n_2} |U_{\mathbf{Q}}^i|^2 \delta(\varepsilon_{n_1, \mathbf{k}-\mathbf{q}} - \varepsilon_{n_2, \mathbf{k}}) I_{q_z} [(1 - \rho_{\mathbf{k}-\mathbf{q}}) T_{n_1} I_{-q_z} T_{n_2} \rho_{\mathbf{k}} - \rho_{\mathbf{k}-\mathbf{q}} T_{n_1} I_{-q_z} T_{n_2} (1 - \rho_{\mathbf{k}})] + h.c. , \\
\partial_t \rho_{\mathbf{k}}|_{\text{ph}} &= \pi \sum_{\mathbf{Q}, n_1, n_2, \lambda} |M_{\mathbf{Q}, \lambda}|^2 I_{q_z} \{ \delta(\varepsilon_{n_1, \mathbf{k}-\mathbf{q}} - \varepsilon_{n_2, \mathbf{k}} + \omega_{\mathbf{Q}, \lambda}) [(N_{\mathbf{Q}, \lambda} + 1)(1 - \rho_{\mathbf{k}-\mathbf{q}}) T_{n_1} I_{-q_z} T_{n_2} \rho_{\mathbf{k}} \\
&\quad - N_{\mathbf{Q}, \lambda} \rho_{\mathbf{k}-\mathbf{q}} T_{n_1} I_{-q_z} T_{n_2} (1 - \rho_{\mathbf{k}})] + \delta(\varepsilon_{n_1, \mathbf{k}-\mathbf{q}} - \varepsilon_{n_2, \mathbf{k}} - \omega_{\mathbf{Q}, \lambda}) [N_{\mathbf{Q}, \lambda} (1 - \rho_{\mathbf{k}-\mathbf{q}}) T_{n_1} I_{-q_z} T_{n_2} \rho_{\mathbf{k}} \\
&\quad - (N_{\mathbf{Q}, \lambda} + 1) \rho_{\mathbf{k}-\mathbf{q}} T_{n_1} I_{-q_z} T_{n_2} (1 - \rho_{\mathbf{k}})] \} + h.c. , \\
\partial_t \rho_{\mathbf{k}}|_{\text{ee}} &= \pi \sum_{\mathbf{q}, q_z, q'_z, \mathbf{k}'} \sum_{n_1, n_2, n_3, n_4} V_{\mathbf{Q}} V_{\mathbf{Q}'} \delta(\varepsilon_{n_1, \mathbf{k}-\mathbf{q}} - \varepsilon_{n_2, \mathbf{k}} + \varepsilon_{n_3, \mathbf{k}'} - \varepsilon_{n_4, \mathbf{k}'-\mathbf{q}}) I_{q_z} \\
&\quad \times \{ (1 - \rho_{\mathbf{k}-\mathbf{q}}) T_{n_1} I_{-q_z} T_{n_2} \rho_{\mathbf{k}} \text{Tr}[(1 - \rho_{\mathbf{k}'}) T_{n_3} I_{q'_z} T_{n_4} \rho_{\mathbf{k}'-\mathbf{q}} I_{-q'_z}] \\
&\quad - \rho_{\mathbf{k}-\mathbf{q}} T_{n_1} I_{-q_z} T_{n_2} (1 - \rho_{\mathbf{k}}) \text{Tr}[\rho_{\mathbf{k}'} T_{n_3} I_{q'_z} T_{n_4} (1 - \rho_{\mathbf{k}'-\mathbf{q}}) I_{-q'_z}] \} + h.c. , \tag{A3}
\end{aligned}$$

in which $[T_{n_1}]_{n, n'} = \delta_{n_1, n} \delta_{n_1, n'}$ and $\mathbf{Q}' = (q_x, q_y, q'_z)$. N_i is the density of impurities, and $|U_{\mathbf{Q}}^i|^2$ is the screened impurity potential. $|M_{\mathbf{Q}, \lambda}|^2$ and $N_{\mathbf{Q}, \lambda} = [\exp(\omega_{\mathbf{Q}, \lambda}/k_B T) - 1]^{-1}$ are the matrix elements of the electron-phonon interaction and the Bose distribution function respectively. $\omega_{\mathbf{Q}, \lambda}$ is the phonon energy spectrum. For the electron-

phonon scattering, we only include electron AC-phonon scattering, for which the explicit expressions can be found in Refs. 25 and 26. The electron-optical phonon scattering is ignored for that the optical phonon energies are around 70 meV and are out of our temperature range.²⁸

* Author to whom correspondence should be addressed; Electronic address: jlcheng@mail.ustc.edu.cn.

- ¹ Ü. Özgür, Ya. I. Alivov, C. Liu, A. Teke, M. A. Reshchikov, S. Doğan, V. Avrutin, S.-J. Cho, and H. Morkoc, *J. Appl. Phys.* **98**, 041301 (2005).
- ² S. Ghosh, V. Sih, W. H. Lau, D. D. Awschalom, S.-Y. Bae, S. Wang, S. Vaidya, and G. Chapline, *Appl. Phys. Lett.* **86**, 232507 (2005); S. Ghosh, D. W. Steuerman, B. Maertz, K. Ohtani, Huaizhe Xu, H. Ohno, and D. D. Awschalom, *Appl. Phys. Lett.* **92**, 162109 (2008).
- ³ W. K. Liu, K. M. Whitaker, A. L. Smith, K. R. Kittilstved, B. H. Robinson, and D. R. Gamelin, *Phys. Rev. Lett.* **98**, 186804 (2007).
- ⁴ D. Lagarde, A. Balocchi, P. Renucci, H. Carrère, T. Amand, X. Marie, Z. X. Mei, and X. L. Du, *Phys. Rev. B* **79**, 045204 (2009); D. Lagarde, A. Balocchi, P. Renucci, H. Carrère, F. Zhao, T. Amand, X. Marie, Z. X. Mei, X. L. Du, and Q. K. Xue, *ibid.* **78**, 033203 (2008).
- ⁵ T. Dietl, H. Ohno, F. Matsukura, J. Cibert, and D. Ferrand, *Science* **287**, 1019 (2000).
- ⁶ N. J. Harmon, W. O. Putikka, and R. Joynt, *Phys. Rev. B* **79**, 115204 (2009).
- ⁷ M. I. D'yakonov and V. I. Perel', *Zh. Eksp. Teor. Fiz.* **60**, 1954 (1971); *Fiz. Tverd. Tela (Leningrad)* **13**, 3581 (1971); *Sov. Phys. JETP* **33**, 1053 (1971); *Sov. Phys. Solid State* **13**, 3023 (1972).
- ⁸ J. H. Jiang and M. W. Wu, *Phys. Rev. B* **79**, 125206 (2009).
- ⁹ J. Zhou, J. L. Cheng and M. W. Wu, *Phys. Rev. B* **75**,

- 045305 (2007); J. Zhou and M. W. Wu, *ibid.* **77**, 075318 (2008).
- ¹⁰ J. Y. Fu and M. W. Wu, *J. Appl. Phys.* **104**, 093712 (2008).
- ¹¹ L. C. Lew Yan Voon, M. Willatzen, M. Cardona, and N. E. Christensen, *Phys. Rev. B* **53**, 10703 (1996).
- ¹² I. Žutić, J. Fabian, and S. Das Sarma, *Rev. Mod. Phys.* **76**, 323 (2004).
- ¹³ M. W. Wu and C. Z. Ning, *Eur. Phys. J. B* **18**, 373 (2000); M. W. Wu, *J. Phys. Soc. Jpn.* **70**, 2195 (2001).
- ¹⁴ M. Q. Weng and M. W. Wu, *Phys. Rev. B* **68**, 075312 (2003); *ibid.* **70**, 195318 (2004).
- ¹⁵ M. Q. Weng, M. W. Wu, and L. Jiang, *Phys. Rev. B* **69**, 245320 (2004).
- ¹⁶ M. M. Glazov and E. L. Ivchenko, *Pis'ma Zh. Eksp. Teor. Fiz.* **75**, 476 (2002); *JETP Lett.* **75**, 403 (2002); *Zh. Eksp. Teor. Fiz.* **126**, 1465 (2004); *JETP* **99**, 1279 (2004).
- ¹⁷ M. M. Glazov, *Phys. Solid State* **45**, 1162 (2003).
- ¹⁸ W. J. H. Leyland, G. H. John, R. T. Harley, M. M. Glazov, E. L. Ivchenko, D. A. Ritchie, I. Farrer, A. J. Shields, and M. Henini, *Phys. Rev. B* **75**, 165309 (2007).
- ¹⁹ Y. Yafet, *Phys. Rev.* **85** 478 (1952); R. J. Elliott, *ibid.* **96**, 266 (1954).
- ²⁰ G. L. Bir, A. G. Aronov, and G. E. Pikus, *Zh. Eksp. Teor. Fiz.* **69**, 1382 (1975); *Sov. Phys. JETP* **42**, 705 (1976).
- ²¹ D. Stich, J. Zhou, T. Korn, R. Schulz, D. Schuh, W. Wegscheider, M. W. Wu, and C. Schüller, *Phys. Rev. Lett.* **98**, 176401 (2007); *Phys. Rev. B* **76**, 205301 (2007).
- ²² K. Shen, *Chin. Phys. Lett.* **26**, 067201 (2009).
- ²³ H. Haug and A. P. Jauho, *Quantum Kinetics in Trans-*

- port and Optics of Semiconductor* (Springer-Verlag, Berlin, 1996).
- ²⁴ M. W. Wu and H. Metiu, Phys. Rev. B **61**, 2945 (2000).
- ²⁵ B. C. Lee, K. W. Kim, M. Dutta, and M. A. Stroscio, Phys. Rev. B **56**, 997 (1997).
- ²⁶ B. Krummheuer, V. M. Axt, T. Kuhn, I. D'Amico, and F. Rossi, Phys. Rev. B **71**, 235329 (2005).
- ²⁷ G. F. Giuliani and G. Vignale, *Quantum Theory of the Electron Liquid* (Cambridge University Press, Cambridge, England, 2005).
- ²⁸ *Semiconductors*, Landolt-Börnstein, New Series, Vol. 17b, edited by O. Madelung (Springer-Verlag, Berlin, 1987).
- ²⁹ X. Z. Ruan, H. H. Luo, Yang Ji, Z. Y. Xu, and V. Umansky, Phys. Rev. B **77**, 193307 (2008).